

# Comparative cytotoxicity evaluation of lanthanide nanomaterials on mouse and human cell lines with metabolic and DNA-quantification assays<sup>a)</sup>

Boon Chin Heng

*School of Materials Science and Engineering, Nanyang Technological University, Block N4.1, 50 Nanyang Avenue, Singapore 639798, Singapore*

Gautom Kumar Das

*Division of Chemical and Biomolecular Engineering, School of Chemical and Biomedical Engineering, Nanyang Technological University, 62 Nanyang Drive, Singapore 637459, Singapore*

Xinxin Zhao and Lwin-Lwin Ma

*School of Materials Science and Engineering, Nanyang Technological University, Block N4.1, 50 Nanyang Avenue, Singapore 639798, Singapore*

Timothy Thatt-Yang Tan

*Division of Chemical and Biomolecular Engineering, School of Chemical and Biomedical Engineering, Nanyang Technological University, 62 Nanyang Drive, Singapore 637459, Singapore*

Kee Woei Ng<sup>b),c)</sup> and Joachim Say-Chye Loo<sup>b),d)</sup>

*School of Materials Science and Engineering, Nanyang Technological University, Block N4.1, 50 Nanyang Avenue, Singapore 639798, Singapore*

(Received 17 August 2010; accepted 9 September 2010; published 14 December 2010)

Lanthanide nanomaterials are considered a less toxic alternative to quantum dots for bioimaging applications. This study evaluated the cytotoxicity of terbium (Tb)-doped gadolinium oxide ( $Gd_2O_3$ ) and dysprosium oxide ( $Dy_2O_3$ ) nanoparticles exposed to human (BEAS-2B) and mouse (L929) cell lines at a concentration range of 200–2000  $\mu g/ml$  for 48 h. Two assay methods were utilized—WST-8 assay (colorimetric) based on mitochondrial metabolic activity and Pico-Green assay (fluorescence), which measures total DNA content. The authors' data showed that Tb-doped  $Gd_2O_3$  nanoparticles were consistently more toxic than Tb-doped  $Dy_2O_3$  nanoparticles. However, exposure to these nanomaterials caused a decrease in proliferation rate for both cell lines rather than a net loss of viable cells after 48 h of exposure. Additionally, there was some degree of discrepancy observed with the two assay methods. For the mouse L929 cell line, the WST-8 assay yielded consistently lower proliferation rates compared to the Pico-Green assay, whereas the opposite trend was observed for the human BEAS-2B cell line. This could arise because of the differential effects of these nanoparticles on the metabolism of L929 and BEAS-2B cells, which in turn may translate to differences in their postexposure proliferation rates. Hence, the Pico-Green assay could have an advantage over the WST-8 assay because it is not skewed by the differential effects of nanomaterials on cellular metabolism. © 2010 American Vacuum Society. [DOI: 10.1116/1.3494617]

## I. INTRODUCTION

In recent years, there has been growing interest in utilizing nanomaterials fabricated from lanthanides for various bioimaging applications.<sup>1–3</sup> As compared to the semiconductor elements utilized in quantum dots,<sup>4,5</sup> the lanthanides are considerably much less toxic. Previous studies have reported that the  $LD_{50}$  (median lethal dose) of quantum dots are typically a thousandfold more than that of lanthanide nanomaterials.<sup>6–8</sup> Additionally, because some of the lanthanides such as gadolinium (Gd) and dysprosium (Dy) possess paramagnetic properties,<sup>9,10</sup> while others such as ter-

bium (Tb) possess fluorescent properties with multiple excitation/emission wavelengths,<sup>11</sup> these can be combined together in the fabrication of unique composite nanomaterials for multimodal imaging. Of particular interest would be multimodal magnetic resonance imaging (MRI)-optical imaging, in which the high spatial resolution of MRI is synergized with the high sensitivity of fluorescent imaging.<sup>12</sup>

Among the various lanthanides, compounds and chelates of  $Gd^{3+}$  and  $Dy^{3+}$  offer much potential as contrast agents for MRI.<sup>13</sup> It is well known that  $Dy^{3+}$  has the highest effective magnetic moment and hence the highest relaxivity among the lanthanides, whereas all electrons of  $Gd^{3+}$  have parallel spins, which is optimal for MRI scans.<sup>13</sup> The useful paramagnetic properties of these two elements can thus be combined together with the fluorescent properties of terbium<sup>11</sup> in the synthesis of multimodal MRI-optical imaging probes. Indeed, a previous study by our group reported the fabrication

<sup>a)</sup>This paper is part of an In Focus section on Biointerphase Science in Singapore, sponsored by Bruker Optik Southeast Asia, IMRE, the Provost's Office and School of Materials Science and Engineering of Nanyang Technological University, and Analytical Technologies Pte. Ltd.

<sup>b)</sup>Authors to whom correspondence should be addressed.

<sup>c)</sup>Electronic mail: kwng@ntu.edu.sg

<sup>d)</sup>Electronic mail: joachimloo@ntu.edu.sg

of Tb-doped Gd<sub>2</sub>O<sub>3</sub> nanorods,<sup>1</sup> while another study by Norek *et al.*<sup>14</sup> reported the synthesis of Dy<sub>2</sub>O<sub>3</sub> nanoparticles as MRI contrast agents.

We have previously conducted a cell viability study using nanoparticles developed as bioimaging probes, including quantum dots and Tb-doped Y<sub>2</sub>O<sub>3</sub> and iron oxide nanoparticles.<sup>15</sup> The Tb-doped Y<sub>2</sub>O<sub>3</sub> nanoparticles were found to have minimal cytotoxic effects on cell viability,<sup>15</sup> based on Alamar Blue metabolic assay.<sup>16</sup> Nevertheless, there is a lack of study on the potential cytotoxicity of Gd<sub>2</sub>O<sub>3</sub> and Dy<sub>2</sub>O<sub>3</sub> nanoparticles. Because of the mildly toxic nature of Gd<sub>2</sub>O<sub>3</sub> and Dy<sub>2</sub>O<sub>3</sub> nanoparticles, currently used cytotoxicity assessment techniques<sup>15,17</sup> often employ a few days of exposure to these nanomaterials to a cell monolayer, prior to carrying out metabolism-based viability assays such as 3-(4,5-dimethylthiazol-2-yl)-2,5-diphenyltetrazolium bromide (MTT),<sup>18</sup> 3-(4,5-dimethylthiazol-2-yl)-5-(3-carboxymethoxyphenyl)-2-(4-sulphophenyl)-2H-tetrazolium (MTS),<sup>19</sup> 2-(2-methoxy-4-nitrophenyl)-3-(4-nitrophenyl)-5-(2,4-disulphophenyl)-2H-tetrazolium (WST-8),<sup>20</sup> and Alamar Blue.<sup>16</sup> These have a number of drawbacks.

First, there is likely to be much cell proliferation during the extended duration of exposure of the cell to these nanomaterials for a few days, particularly if fast-growing immortalized cell lines are being utilized for cytotoxicity assays. This will obviously skew the data, because even if there is no cell death with nanoparticle exposure, the cell viability assay will still yield differences in cell numbers between the experimental and control group if these nanomaterials have an effect on just the cell proliferation rate. Hence, these currently utilized cytotoxicity assessment protocols fail to distinguish between cell death and cell proliferation, and fallaciously present the final data as an overall loss of cell viability with respect to the untreated negative control. Thus, there is a need to discern whether there is an overall decrease or increase in the absolute numbers of viable cells after exposure to these nanomaterials.

Second, metabolism-based cell viability assays such as MTT,<sup>18</sup> MTS,<sup>19</sup> WST-8,<sup>20</sup> and Alamar Blue<sup>16</sup> may be skewed by the differential effects of various nanomaterials on cellular metabolism. In a previous study by Shappell<sup>21</sup> that assessed ergovaline toxicity on CACO-2 cells, it was reported that the actual decrease in absolute numbers of viable cells was masked by increased cellular metabolism upon exposure to ergovaline and that there were significant discrepancies in the cell viability values measured by DNA-quantification and metabolic assays (i.e., MTT). Hence, there is a need to compare different methods for assessing the cytotoxicity of these lanthanide nanomaterials, in particular, DNA-quantification versus metabolic assays.

Lastly, another major drawback of previously reported studies that assessed the cytotoxicity of these lanthanide nanomaterials is that there was no further investigation of cell biology and physiology after nanoparticle exposure. Given the utility of these lanthanide nanomaterials as bioimaging

probes, it is therefore of clinical importance to evaluate whether the nanoparticles have any adverse postexposure effects.

Hence, this study will attempt to address these various deficiencies by a comparative cytotoxicity evaluation of Tb-doped Gd<sub>2</sub>O<sub>3</sub> and Dy<sub>2</sub>O<sub>3</sub> nanoparticles with metabolic (WST-8) and DNA-quantification assays (Pico-Green), utilizing both a mouse and a human cell line [murine fibroblast cell line (L929) and human bronchial epithelial cell line (BEAS-2B), respectively]. Additionally, the postexposure effects of these nanomaterials on L929 and BEAS-2B cells will be assessed by cell proliferation assays.

## II. MATERIALS AND METHODS

### A. Cell line, culture media, reagents, chemicals, and labware consumables

BEAS-2B and L-929 were purchased from the American Type Culture Collection (ATCC, Manassas, VA). Unless otherwise stated, all reagents and chemicals were purchased from Sigma-Aldrich, Inc. (St. Louis, MO), all culture media, serum, and phosphate buffered saline (PBS) were purchased from Gibco-BRL, Inc. (Gaithersburg, MD), while all labware consumables were purchased from Corning, Inc. (Corning, NY).

### B. Synthesis of Tb-doped Gd<sub>2</sub>O<sub>3</sub> and Dy<sub>2</sub>O<sub>3</sub> nanoparticles

Tb-doped Gd<sub>2</sub>O<sub>3</sub> nanoparticles were synthesized as previously described.<sup>1</sup> Briefly, 2 mmol of Gd<sub>2</sub>O<sub>3</sub> (0.725 g) together with 0.22 mmol (0.082 g) of TbCl<sub>3</sub>·6H<sub>2</sub>O were dissolved in 0.8 ml of 70% (v/v) HNO<sub>3</sub> (Alfa-Aesar, Inc., Ward Hill, MA). 6 ml of H<sub>2</sub>O, 9 ml of ethanol, 15 ml of hexane, and 2–4 ml of oleic acid (Alfa-Aesar, Inc., Ward Hill, MA) were added to this acidic solution in sequence and the mixture was stirred in a closed vessel at 70 °C for 2 h. A second solution containing 0.24 g of NaOH (Fluka Chemical Corp., Milwaukee, WI) dissolved in 6 ml of H<sub>2</sub>O was then added dropwise and heated at 70 °C with stirring for another 4 h. The mixture separated into two transparent layers at this stage. The upper organic layer containing the Gd-Tb-oleate complex was collected, washed with 30 ml of distilled water, and dried overnight in an oven at 70 °C to evaporate water and hexane. The waxy Gd-Tb-oleate obtained after drying was dissolved in 20 ml of oleylamine in a three-neck flask and purged with N<sub>2</sub>. The solution was then heated to 300 °C at a rate of 5 °C/min under the blanket of N<sub>2</sub>. First, nanodots (≈3 × 3 nm<sup>2</sup>) emerged and then nanorods (≈3 × 15 nm<sup>2</sup>) were grown in the solution at different reflux times. The mixture was cooled to room temperature before precipitation and was purified by centrifugation with extensive ethanol washing. The nanoparticles were finally dispersed in cyclohexane for further characterization. For Tb-doped Dy<sub>2</sub>O<sub>3</sub> nanoparticles, 2 mmol of Dy<sub>2</sub>O<sub>3</sub> (0.746 g) were used instead of 2 mmol of Gd<sub>2</sub>O<sub>3</sub>.

Subsequently, amine derivatization of Tb-doped Gd<sub>2</sub>O<sub>3</sub> and Dy<sub>2</sub>O<sub>3</sub> nanorods was performed by following a previ-

ously adopted procedure.<sup>22</sup> Surface amine groups were used as they were found to have minimal cytotoxicity.<sup>3</sup> In a typical procedure, reverse micelles were first prepared by dissolving 0.2 g of Igepal CO-520 [polyoxyethylene (5) nonylphenyl ether] in 4 ml of cyclohexane, followed by vigorous stirring for 30 min. Meanwhile, the Tb-doped Gd<sub>2</sub>O<sub>3</sub> or Dy<sub>2</sub>O<sub>3</sub> nanorods were redispersed in chloroform at a concentration of 4 mg/ml and 1 ml was added to the micelle solution and stirred for 15 min. Subsequently, 30  $\mu$ l of 3-aminopropyltrimethoxysilane (APS; Fluka Chemical Corp., Milwaukee, WI) were added and the mixture was stirred for another 1 h. Then, 30  $\mu$ l of 25% (w/v) tetramethylammonium hydroxide (TMAH) in methanol were added. After an additional 1 h of stirring, 20  $\mu$ l of de-ionized water were added and stirred for 30 min. At this stage, globules of silanized nanorods were formed and settled at the bottom of the flask, leaving the upper solution transparent. The transparent organic phase was then discarded and the globules were then collected. After this, the nanorods were washed with chloroform and ethanol for the complete removal of excess surfactant and other reactants, and were finally dispersed in de-ionized water. Silanization of the Tb-doped Gd<sub>2</sub>O<sub>3</sub> and Dy<sub>2</sub>O<sub>3</sub> nanodots was performed using the same process but with 25  $\mu$ l of APS, 25  $\mu$ l TMAH, and 15  $\mu$ l of de-ionized water.

### C. Transmission electron microscopy characterization of nanoparticles

Transmission electron microscopy (TEM) micrographs of the Tb-doped Gd<sub>2</sub>O<sub>3</sub> and Dy<sub>2</sub>O<sub>3</sub> nanoparticles were acquired using a JEOL JEM-2100F microscope operating at 200 kV. A drop of nanoparticle dispersion was placed onto a holey carbon film supported on a 200 mesh copper grid (3 mm in diameter) and allowed to dry in air at room temperature. The carbon grid with sample was then mounted into the vacuum chamber for TEM imaging.

### D. Dynamic light scattering (DLS) measurement of hydrodynamic size within cell culture medium

The hydrodynamic size of Tb-doped Gd<sub>2</sub>O<sub>3</sub> and Dy<sub>2</sub>O<sub>3</sub> nanoparticles within a colloidal suspension in a cell culture medium [Dulbecco's minimum essential medium (DMEM) supplemented with 10% (v/v) fetal bovine serum (FBS)] was measured by DLS utilizing a Brookhaven 90 Plus particle size analyzer fitted with a 15 mW solid state laser (Brookhaven Instruments Corporation, Inc., Holtsville, NY). DLS measurement was carried out on colloidal suspensions of all three nanoparticles at 200 and 2000  $\mu$ g/ml, which were the lowest and the highest concentrations that cells were exposed to in this study. The nanoparticle suspension in culture medium was sonicated for 30 min with an ultrasonic cleaner (MRC Laboratory Instruments, Inc., Holon, Israel) prior to being utilized for DLS measurement.

### E. Preparation of monolayers of L929 and BEAS-2B cells for cytotoxicity studies

L929 and BEAS-2B cells were seeded on 12-well culture plates ( $\approx 4.8$  cm<sup>2</sup> per well) at a density of  $5.0 \times 10^4$  cells per well. The culture media were composed of DMEM supplemented with 10% (v/v) FBS and 1% (v/v) antibiotic-antimycotic solution (Cat No. A5955, Sigma-Aldrich, Inc.). The seeded cells were then cultured for 24 h prior to being utilized for cytotoxicity assays. Concurrently, on day 1 after seeding, the newly seeded monolayers of L929 and BEAS-2B cells were also subjected to the WST-8 and Pico-Green assays, which were subsequently described.

### F. Exposure of L929 and BEAS-2B cell monolayers to Tb-doped Gd<sub>2</sub>O<sub>3</sub> and Dy<sub>2</sub>O<sub>3</sub> nanoparticles

The following day after seeding (day 1), monolayers of L929 and BEAS-2B cells were exposed to varying concentrations (0, 200, 400, 1000, and 2000  $\mu$ g/ml) of Tb-doped Gd<sub>2</sub>O<sub>3</sub> nanorods ( $\approx 3 \times 15$  nm<sup>2</sup>) and nanodots ( $\approx 3 \times 3$  nm<sup>2</sup>) as well as Tb-doped Dy<sub>2</sub>O<sub>3</sub> nanorods ( $\approx 3 \times 15$  nm<sup>2</sup>) constituted in DMEM media (0.5 ml) supplemented with 10% (v/v) FBS and 1% (v/v) antibiotic-antimycotic solution (Cat No. A5955, Sigma-Aldrich, Inc.) for a duration of 48 h at 37 °C within a 5% CO<sub>2</sub> incubator. Prior to incubation with either L929 or BEAS-2B cells, concentrated suspensions of all three nanoparticles at 20 mg/ml in de-ionized water were placed within a Petri dish and sterilized by exposure to UV irradiation for 30 min. This was followed by 1:10 dilution with culture media to yield a working concentration of 2000  $\mu$ g/ml, which was in turn serially diluted to other working concentrations of 1000, 400, and 200  $\mu$ g/ml. A 1:10 mixture of de-ionized water with culture media was utilized for all serial dilutions as well as for the zero concentration control. All working concentrations of nanoparticle suspensions (200, 400, 1000, and 2000  $\mu$ g/ml) were sonicated for 30 min within an ultrasonic cleaner (MRC Laboratory Instruments, Inc., Holon, Israel) prior to being utilized for experiments. Altogether, there were four replicates for each different nanoparticle type and concentration within the experimental and control groups. The cells were subjected to the WST-8 assay<sup>20</sup> before (day 1) and after 48 h of culture (day 3), so as to quantify the increase/decrease in total number of viable cells and the proliferation rate after exposure to varying concentrations of Gd<sub>2</sub>O<sub>3</sub> and Dy<sub>2</sub>O<sub>3</sub> nanoparticles for 48 h.

### G. WST-8 assay for assessing cell viability and proliferation rate after exposure to the Tb-doped Gd<sub>2</sub>O<sub>3</sub> and Dy<sub>2</sub>O<sub>3</sub> nanoparticles

The WST-8 assay for cell viability<sup>20</sup> was carried out with the cell counting kit solution (CCK-8 kit, Cat No. CK04-11) from Dojindo Molecular Laboratories, Inc. (Kumamoto, Japan). The CCK-8 kit utilizes the water-soluble tetrazolium salt WST-8 [2-(2-methoxy-4-nitrophenyl)-3-(4-nitrophenyl)-5-(2,4-disulphophenyl)-2H-tetrazolium, monosodium salt] in measuring Nicotinamide Adenine Dinucleotide, reduced

form (NADH) production resulting from the dehydrogenase activity of viable cells. The subsequent reduction of WST-8 by viable cells produces an orange-colored formazan product with an absorbance at 450 nm. The cells were washed three times in PBS, prior to the addition of 25  $\mu$ l of CCK-8 solution and 225  $\mu$ l of culture media within each well of the 12-well culture plate. After incubation for 1 h at 37 °C within a 5% CO<sub>2</sub> incubator, 100  $\mu$ l aliquots of the reaction mixture were transferred onto a fresh 96-well plate, and absorbance readings were measured spectrophotometrically at 450 nm using an Infinite200<sup>®</sup> microplate reader (Tecan, Inc., Maennedorf, Switzerland). The cell proliferation index after exposure to varying concentrations of Gd<sub>2</sub>O<sub>3</sub> and Dy<sub>2</sub>O<sub>3</sub> nanoparticles for 48 h was calculated as the ratio of absorbance readings (450 nm) before and after nanoparticle exposure, on day 1 and day 3, respectively, after correction for blank absorbance reading of the reaction mixture incubated without cells for the same duration (1 h) at 37 °C. As an alternative means of data presentation, the percentage of viable cells was also calculated as the ratio of absorbance readings (450 nm) yielded by the treated and untreated (negative control) wells.

#### H. Pico-Green assay for assessing cell proliferation rate by DNA quantification

Following the WST-8 assay, the L929 and BEAS-2B cells that were exposed to the higher concentrations of the Tb-doped Gd<sub>2</sub>O<sub>3</sub> and Dy<sub>2</sub>O<sub>3</sub> nanoparticles (1000 and 2000  $\mu$ g/ml) were washed three times in PBS, prior to being lysed with 0.1% (v/v) Triton X-100 solution with gentle pipetting for a duration of 30 min (0.5 ml per well of the 12-well plate). The Pico-Green working solution was then prepared by diluting the concentrated Pico-Green reagent in Tris-EDTA (TE) buffer (10 mM Tris, 1 mM ethylenediamine tetra-acetic acid, and pH 7.4) at a dilution ratio of 1:200 according to the manufacturer's instructions (Quant-iT<sup>®</sup> PicoGreen kit, Cat No. P7589; Invitrogen, Inc., Carlsbad, CA). Subsequently, the cell-lysate was mixed with the Pico-Green working solution at a 1:1 ratio (100  $\mu$ l within each well of a 96-well plate) and incubated for at least 10 min at room temperature prior to reading the fluorescence emission at 520 nm under an excitation wavelength of 480 nm with an Infinite200<sup>®</sup> microplate reader (Tecan, Inc., Maennedorf, Switzerland). The cell proliferation index after exposure to varying concentrations of Gd<sub>2</sub>O<sub>3</sub> and Dy<sub>2</sub>O<sub>3</sub> nanoparticles for 48 h was calculated as the ratio of fluorescence readings (520 nm) before and after nanoparticle exposure, on day 1 and day 3, respectively, after correction for blank fluorescence reading of the Pico-Green working solution incubated with 0.1% Triton X-100 without lysed cells. The calculation of proliferation index based on the ratio of blank-corrected fluorescence readings in the Pico-Green assay is valid because the cell densities and corresponding DNA concentrations quantified in this study lay within the linear range of the assay kit (Quant-iT<sup>®</sup> PicoGreen kit; Invitrogen, Inc., Carlsbad, CA), which extends over more than four orders of magnitude in DNA concentration, from 25 pg/ml to 1000

ng/ml, according to the manufacturer's specification.

#### I. Assessment of postexposure proliferation rates

L929 and BEAS-2B cells were seeded within T25 tissue-culture flasks at a density of  $2.5 \times 10^5$  cells per flask, and 24 h later were exposed to 2000  $\mu$ g/ml of Tb-doped Gd<sub>2</sub>O<sub>3</sub> nanorods ( $\approx 3 \times 15$  nm<sup>2</sup>) and nanodots ( $\approx 3 \times 3$  nm<sup>2</sup>) as well as Tb-doped Dy<sub>2</sub>O<sub>3</sub> nanorods ( $\approx 3 \times 15$  nm<sup>2</sup>) for a total duration of 48 h. Subsequently, the cells were trypsinized and replated on either glass cover slips or 12-well culture dishes at a seeding density of  $5.0 \times 10^4$  cells per well (0.5 ml of culture medium per well). On day 1 and day 3 after seeding, the monolayers of L929 and BEAS-2B cells that were pre-exposed to the Tb-doped Gd<sub>2</sub>O<sub>3</sub> and Dy<sub>2</sub>O<sub>3</sub> nanoparticles were subjected to both the WST-8 and Pico-Green assays as previously described, so as to determine the postexposure proliferation rates. At the same time, the pre-exposed L929 and BEAS-2B cells that were replated on glass cover slips were imaged 24 h later under fluorescent confocal microscopy (Leica TCS SP5; Leica Microsystems GmbH, Wetzlar, Germany) at an excitation wavelength of 235 nm and emission wavelengths of 485 and 585 nm for qualitative assessment of nanoparticle uptake by the cells.

#### J. Statistical analysis of data

The results from each data set were expressed as mean  $\pm$  standard derivations ( $n=4$  for all data sets). Statistical differences between data sets were assessed by the student's t-test, with a P-value of less than 0.05 being considered significantly different.

### III. RESULTS

#### A. Transmission electron microscopy characterization of nanoparticles

The TEM micrographs of the Tb-doped Gd<sub>2</sub>O<sub>3</sub> and Dy<sub>2</sub>O<sub>3</sub> nanoparticles are shown in Fig. 1. As seen in Figs. 1(A) and 1(C), the dimensions of both the Tb-doped Gd<sub>2</sub>O<sub>3</sub> and Dy<sub>2</sub>O<sub>3</sub> nanorods are approximately  $3 \times 15$  nm<sup>2</sup> [Figs. 1(A) and 1(C), respectively], whereas the dimensions of the Tb-doped Gd<sub>2</sub>O<sub>3</sub> nanodots are approximately  $3 \times 3$  nm<sup>2</sup> [Fig. 1(B)].

#### B. DLS measurement of hydrodynamic size within a cell culture medium

According to the particle size distribution plots (Fig. 2), the hydrodynamic size range of Tb-doped Gd<sub>2</sub>O<sub>3</sub> and Dy<sub>2</sub>O<sub>3</sub> nanoparticles within a culture medium is similar to the results observed with TEM (Fig. 1), thus indicating that these nanoparticles are relatively stable in a culture medium. However, the distribution plots do show a slight shift toward bigger particle size at the higher concentration of 2000 vs 200  $\mu$ g/ml, which suggests some degree of particle aggregation with increasing concentration. Nevertheless, the aggregated particles are still within the acceptable nanosize range (<100 nm).

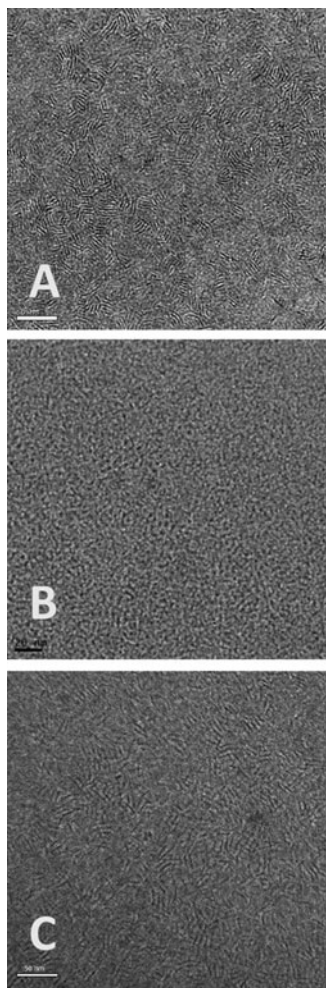


FIG. 1. TEM images of (A)  $\text{Gd}_2\text{O}_3$  nanorods ( $\approx 3 \times 15 \text{ nm}^2$ ), (B)  $\text{Gd}_2\text{O}_3$  nanodots ( $\approx 3 \times 3 \text{ nm}^2$ ), and (C)  $\text{Dy}_2\text{O}_3$  nanorods ( $\approx 3 \times 15 \text{ nm}^2$ ).

### C. WST-8 assay on L929 and BEAS-2B cells exposed to increasing concentrations of Tb-doped $\text{Gd}_2\text{O}_3$ and $\text{Dy}_2\text{O}_3$ nanoparticles

After 48 h exposure to increasing concentrations (200, 400, 1000, and 2000  $\mu\text{g}/\text{ml}$ ) of Tb-doped  $\text{Gd}_2\text{O}_3$  and  $\text{Dy}_2\text{O}_3$  nanoparticles, the L929 monolayers were subjected to the WST-8 assay, and the results are presented in two alternative formats: first, in terms of percentage cell viability [Figs. 3(A) and 4(A)], and second, in terms of proliferation index over 48 h [Figs. 3(B) and 4(B)]. The overall trend and shape of the graphs appear to be similar with the two alternative presentation formats, except that when the data were plotted as proliferation index [Figs. 3(B) and 4(B)], it was obvious that there was no net decrease in the absolute number of viable cells for both L929 and BEAS-2B after 48 h of exposure to increasing concentrations of nanoparticles, since the proliferation index value was consistently above 1 for the entire concentration range examined. This fact is not apparent if the data were more conventionally plotted as percentage cell viability [Figs. 3(A) and 4(A)].

With L929 cells [Figs. 3(A) and 3(B)], it was observed that the  $\text{Gd}_2\text{O}_3$  nanodots were consistently more toxic than

the  $\text{Gd}_2\text{O}_3$  nanorods and that the  $\text{Dy}_2\text{O}_3$  nanorods were consistently less toxic than both the  $\text{Gd}_2\text{O}_3$  nanodots and the  $\text{Gd}_2\text{O}_3$  nanorods. All data points for the three different nanoparticles were significantly different from each other ( $P < 0.05$ ), except at the lowest concentration point of 200  $\mu\text{g}/\text{ml}$ .

With BEAS-2B cells [Figs. 4(A) and 4(B)], it was also observed that the  $\text{Dy}_2\text{O}_3$  nanorods were consistently less toxic than both the  $\text{Gd}_2\text{O}_3$  nanodots and the  $\text{Gd}_2\text{O}_3$  nanorods. Nevertheless, there was some degree of overlap with respect to the cytotoxicity of  $\text{Gd}_2\text{O}_3$  nanodots and nanorods. At the higher concentrations of 1000 and 2000  $\mu\text{g}/\text{ml}$ , the  $\text{Gd}_2\text{O}_3$  nanodots were significantly more toxic than  $\text{Gd}_2\text{O}_3$  nanorods ( $P < 0.05$ ), which is consistent with the previous trend observed for L929 cells [Figs. 3(A) and 3(B)]. The trend was, however, reversed at 400  $\mu\text{g}/\text{ml}$ , probably due to some degree of experimental variability. All data points for the three different nanoparticles were significantly different from each other ( $P < 0.05$ ), except at the lowest concentration point of 200  $\mu\text{g}/\text{ml}$ , where there were no significant differences in the toxicity of  $\text{Gd}_2\text{O}_3$  nanorods and nanodots, but with the  $\text{Dy}_2\text{O}_3$  nanorods still being significantly less toxic than both the  $\text{Gd}_2\text{O}_3$  nanorods and the  $\text{Gd}_2\text{O}_3$  nanodots.

### D. Pico-Green assay on L929 and BEAS-2B cells exposed to higher concentrations (1000 and 2000 $\mu\text{g}/\text{ml}$ ) of Tb-doped $\text{Gd}_2\text{O}_3$ and $\text{Dy}_2\text{O}_3$ nanoparticles

As seen in Fig. 5, upon carrying out the Pico-Green assay (DNA quantification) on L929 cells exposed to 1000 and 2000  $\mu\text{g}/\text{ml}$  of Tb-doped  $\text{Gd}_2\text{O}_3$  and  $\text{Dy}_2\text{O}_3$  nanoparticles, the data trend was similar to that obtained with the WST-8 assay, with the  $\text{Gd}_2\text{O}_3$  nanodots being consistently more toxic than the  $\text{Gd}_2\text{O}_3$  nanorods and with the  $\text{Dy}_2\text{O}_3$  nanorods being consistently less toxic than both the  $\text{Gd}_2\text{O}_3$  nanodots and the  $\text{Gd}_2\text{O}_3$  nanorods. Additionally, it was again observed that there was no net decrease in the number of viable cells upon exposure of L929 to these nanoparticles, since the values of proliferation index obtained with the Pico-Green assay was consistently above 1. Nevertheless, it was observed that the values of proliferation index (48 h) obtained with the Pico-Green assay were consistently higher than the corresponding values of proliferation index obtained with the WST-8 assay (Fig. 5). This could imply that the exposure of L929 cells to the  $\text{Gd}_2\text{O}_3$  and  $\text{Dy}_2\text{O}_3$  nanoparticles could somehow slow down the metabolic activity of these cells.

However, in the case of BEAS-2B cells (Fig. 6), the opposite trend was observed, with the Pico-Green assay yielding consistently lower values of proliferation index than the WST-8 assay. This could in turn imply that the  $\text{Gd}_2\text{O}_3$  and  $\text{Dy}_2\text{O}_3$  nanoparticles had differential effects on the cellular metabolism of different cell types, increasing the metabolic activity of BEAS-2B cells while slowing down the metabolism of L929 cells. With the Pico-Green assay, a similar trend of the  $\text{Dy}_2\text{O}_3$  nanorods being consistently less toxic than both the  $\text{Gd}_2\text{O}_3$  nanodots and the  $\text{Gd}_2\text{O}_3$  nanorods was ob-

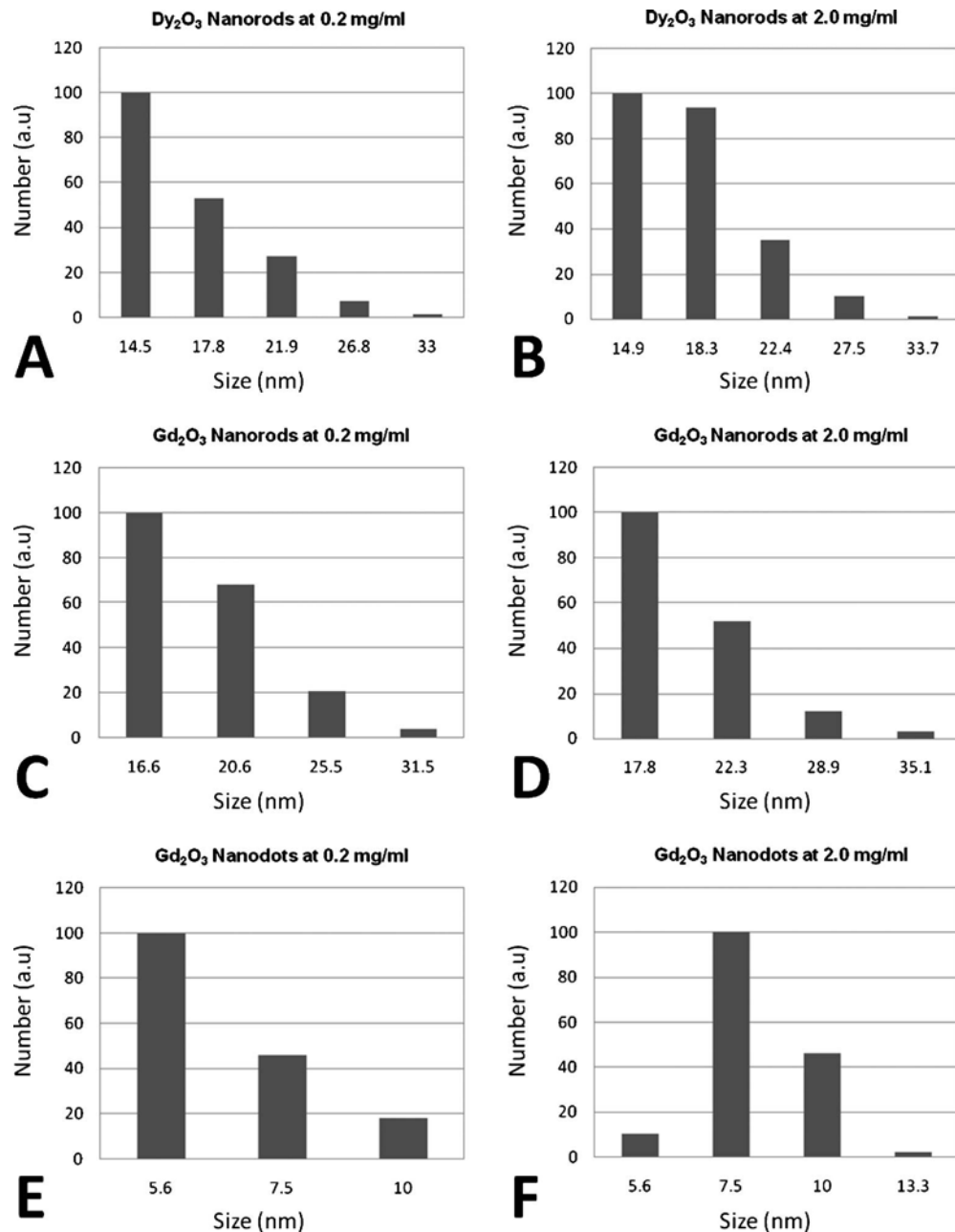


FIG. 2. Size distribution plots of (A) Dy<sub>2</sub>O<sub>3</sub> nanorods at 0.2 mg/ml, (B) Dy<sub>2</sub>O<sub>3</sub> nanorods at 2.0 mg/ml, (C) Gd<sub>2</sub>O<sub>3</sub> nanorods at 0.2 mg/ml, (D) Gd<sub>2</sub>O<sub>3</sub> nanorods at 2.0 mg/ml, (E) Gd<sub>2</sub>O<sub>3</sub> nanodots at 0.2 mg/ml, and (F) Gd<sub>2</sub>O<sub>3</sub> nanodots at 2.0 mg/ml, as determined by DLS.

served. However, no significant differences between the toxicity of Gd<sub>2</sub>O<sub>3</sub> nanodots and nanorods on BEAS-2B cells were observed with the Pico-Green assay.

Interestingly, for the untreated controls of both L929 and BEAS-2B cells (Figs. 5 and 6), the WST-8 assay consistently yielded significantly higher ( $P < 0.05$ ) values of proliferation index compared to the WST-8 assay. This would thus imply that in the absence of toxic challenge, the cellular metabolism of both L929 and BEAS-2B cells exhibited an increase, from day 1 to day 3, after seeding.

### E. Assessment of postexposure proliferation rates

As seen in Figs. 7 and 8, confocal microscopy confirmed the presence of Gd<sub>2</sub>O<sub>3</sub> and Dy<sub>2</sub>O<sub>3</sub> nanoparticles within the

cytoplasm of L929 and BEAS-2B cells, respectively, 24 h after trypsinization and reseeding onto new culture plates following 48 h exposure to 2000  $\mu\text{g/ml}$  of Tb-doped Gd<sub>2</sub>O<sub>3</sub> and Dy<sub>2</sub>O<sub>3</sub> nanoparticles. Although the fluorescence emission wavelength utilized in Figs. 7 and 8 are different (485 and 585 nm, respectively), it must be noted that the Tb-doped Gd<sub>2</sub>O<sub>3</sub> and Dy<sub>2</sub>O<sub>3</sub> nanoparticles can emit fluorescence at both wavelengths upon excitation at 235 nm.

Upon assessment of the postexposure proliferation rate of L929 cells with both WST-8 and Pico-Green assay (Fig. 9), it was observed that prior exposure to Gd<sub>2</sub>O<sub>3</sub> nanodots and Dy<sub>2</sub>O<sub>3</sub> nanorods for 48 h led to a marginal but significant ( $p < 0.05$ ) decrease in the postexposure proliferation index (48 h) with respect to the unexposed control. There was,

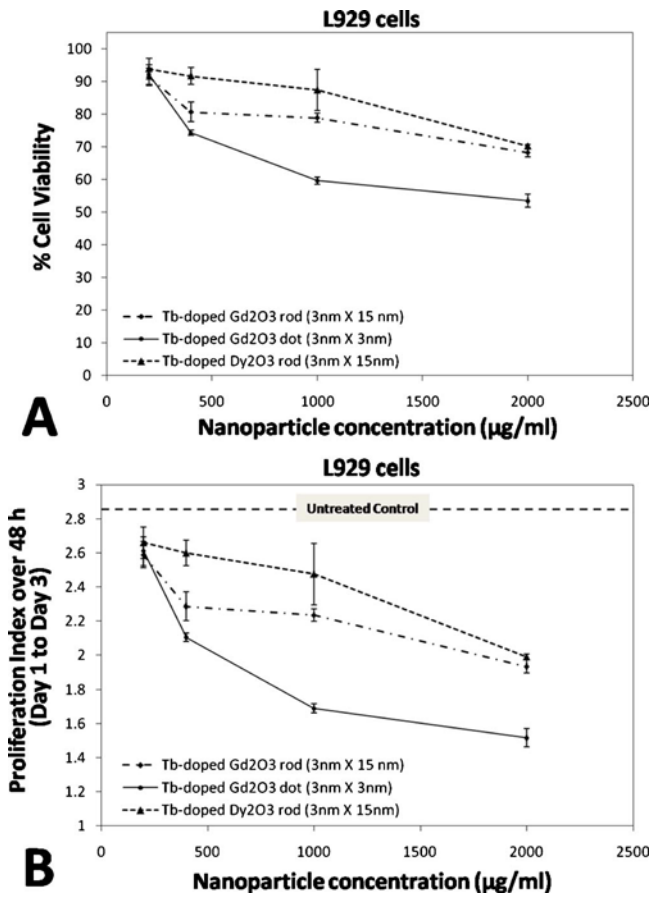


Fig. 3. (Color online) Assessment of Gd<sub>2</sub>O<sub>3</sub> and Dy<sub>2</sub>O<sub>3</sub> nanoparticle cytotoxicity on L929 cells with WST-8 assay. The data were conventionally presented as (A) % cell viability and (B) proliferation index over 48 h (day 1 to day 3).

however, no significant difference between the postexposure proliferation index of the Gd<sub>2</sub>O<sub>3</sub> nanorod and the unexposed control.

The opposite trend was, however, observed with BEAS-2B cells. As seen in Fig. 10, prior exposure to Gd<sub>2</sub>O<sub>3</sub> nanodots and Dy<sub>2</sub>O<sub>3</sub> nanorods for 48 h led instead to an increase in the postexposure proliferation index (48 h) with respect to the unexposed control, in the case of all three nanoparticles, as assessed by both WST-8 and Pico-Green assays. All differences were statistically significant ( $P < 0.05$ ), with the exception of the data point for the Gd<sub>2</sub>O<sub>3</sub> nanorod assessed by the Pico-Green assay.

Interestingly, it was observed that the values of proliferation index obtained with the Pico-Green assay were consistently and significantly lower ( $P < 0.05$ ) than the corresponding values obtained by the WST-8 assay for BEAS-2B cells (Fig. 10). This was, however, not observed for L929 cells (Fig. 9).

#### IV. DISCUSSION

The overwhelming majority of previous studies on the toxicology of nanomaterials utilized metabolic assays such as MTT,<sup>18</sup> MTS,<sup>19</sup> WST-8,<sup>20</sup> and Alamar Blue,<sup>16</sup> and conven-

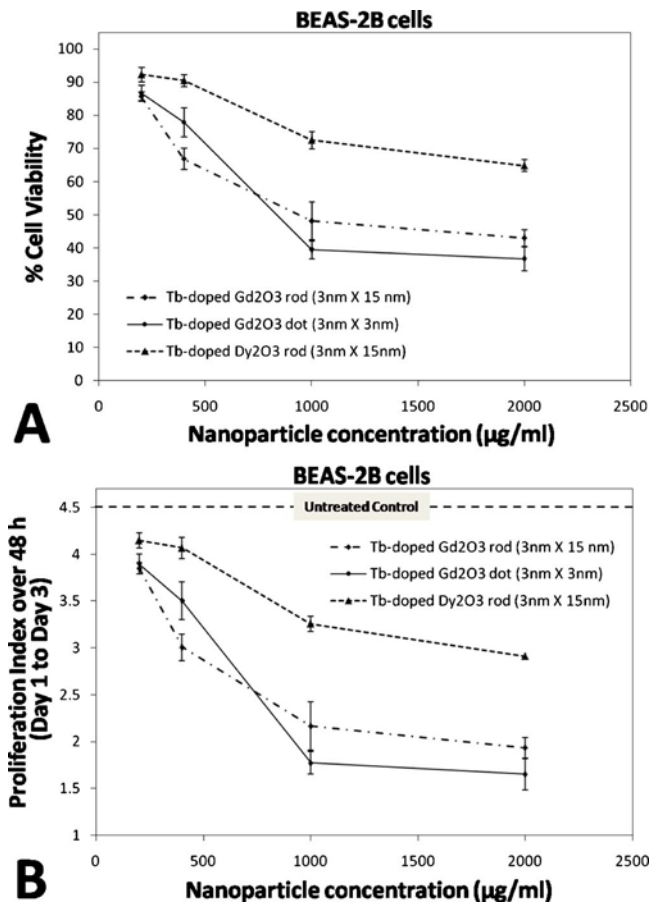


Fig. 4. (Color online) Assessment of Gd<sub>2</sub>O<sub>3</sub> and Dy<sub>2</sub>O<sub>3</sub> nanoparticle cytotoxicity on BEAS-2B cells with WST-8 assay. The data were conventionally presented as (A) % cell viability and (B) proliferation index over 48 h (day 1 to day 3).

tionally present cytotoxicity data in terms of loss of cell viability. This may be inappropriate for mildly toxic nanomaterials that require a longer duration of cellular exposure for cytotoxic effects to become apparent. In particular, the data may be skewed by cell proliferation during the prolonged duration of exposure (i.e., 2 to 3 days) to these mildly toxic

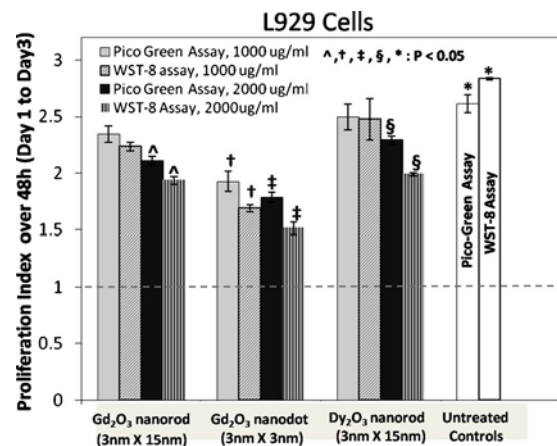


Fig. 5. (Color online) Comparative evaluation of the cytotoxicity of Gd<sub>2</sub>O<sub>3</sub> and Dy<sub>2</sub>O<sub>3</sub> nanoparticles on L929 cells with Pico-Green and WST-8 assays.

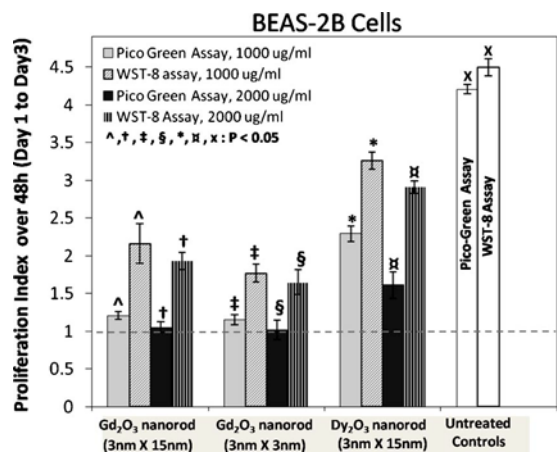


Fig. 6. (Color online) Comparative evaluation of the cytotoxicity of Gd<sub>2</sub>O<sub>3</sub> and Dy<sub>2</sub>O<sub>3</sub> nanoparticles on BEAS-2B cells with Pico-Green and WST-8 assays.

nanomaterials<sup>15,17</sup> if fast-growing immortalized cell lines are being utilized for these assays. Hence, this study compared two alternative formats of presenting cytotoxicity data in terms of proliferation index versus cell viability. At the same time, the relatively mild toxicity of lanthanide nanomaterials<sup>4-6</sup> would necessitate us to examine much higher concentrations, so that a greater and more significant change in cell proliferation rate or viability would be displayed in our experimental data. In this study, we investigated the cytotoxicity of lanthanide nanomaterials at extremely high concentrations of up to 1 and 2 mg/ml, much higher than that normally utilized in biomedical applications. By contrast, in our previous study,<sup>15</sup> the highest concentration examined was only 0.25 mg/ml. Even so, a dosage of 0.25 mg/ml is nearly double of that used by Jaiswal *et al.*<sup>23</sup> for the labeling of HeLa cells and approximately 60 times higher than the concentrations used by Wu *et al.*<sup>24</sup> for targeting Her2 epitopes on breast cancer cells.

As seen in the results (Figs. 3 and 4), it is obvious that there was no net decrease in the absolute number of viable

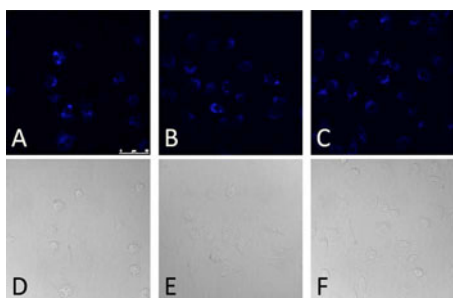


Fig. 7. (Color online) Confocal fluorescent microscopy images of L929 cells, 24 h after trypsinization and reseeding on new culture plates, following 48 h of pre-exposure to 2000 µg/ml of Gd<sub>2</sub>O<sub>3</sub> and Dy<sub>2</sub>O<sub>3</sub> nanoparticles. (A)–(C) Fluorescent images of L929 cells that were pre-exposed to Gd<sub>2</sub>O<sub>3</sub> nanorods (≈3×15 nm<sup>2</sup>), Gd<sub>2</sub>O<sub>3</sub> nanodots (≈3×3 nm<sup>2</sup>), and Dy<sub>2</sub>O<sub>3</sub> nanorods, respectively. (D)–(F) Corresponding bright-field images of (A)–(C). The excitation wavelength was 235 nm, while the emission wavelength was 485 nm.

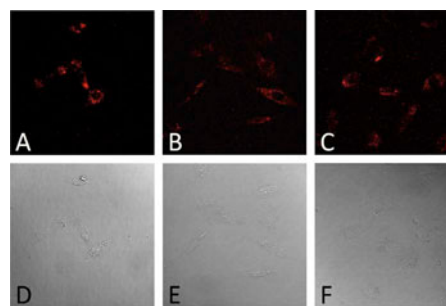


Fig. 8. (Color online) Confocal fluorescent microscopy images of BEAS-2B cells, 24 h after trypsinization and reseeding on new culture plates, following 48 h of pre-exposure to 2000 µg/ml of Gd<sub>2</sub>O<sub>3</sub> and Dy<sub>2</sub>O<sub>3</sub> nanoparticles. (A)–(C) Fluorescent images of BEAS-2B cells that were pre-exposed to Gd<sub>2</sub>O<sub>3</sub> nanorods (≈3×15 nm<sup>2</sup>), Gd<sub>2</sub>O<sub>3</sub> nanodots (≈3×3 nm<sup>2</sup>), and Dy<sub>2</sub>O<sub>3</sub> nanorods, respectively. (D)–(F) Corresponding bright-field images of (A)–(C). The excitation wavelength was 235 nm, while the emission wavelength was 585 nm.

cells after 48 h exposure to the Tb-doped Gd<sub>2</sub>O<sub>3</sub> and Dy<sub>2</sub>O<sub>3</sub> nanoparticles, when cytotoxicity data were presented in terms of proliferation index [Figs. 3(B) and 4(B)]. This particular information is obscured when the data were more conventionally presented in terms of loss of cell viability [Figs. 3(A) and 4(A)]. This in turn causes us to rethink whether the conventional data presentation format in terms of cell viability loss is still appropriate for the diverse array of nanomaterials being investigated.

When the cytotoxicity data were conventionally presented as percentage cell viability [Figs. 3(A) and 4(A)], it was necessary to carry out assay readings (both WST-8 and Pico-Green) only at the end point on day 3, and the results were compared only with the untreated control on day 3. By contrast, when the data were instead expressed as proliferation index [Figs. 3(B) and 4(B)], it was necessary to carry out assay readings on both day 1 and day 3, and the results were compared with the untreated control on both day 1 and day 3. Hence, it is evident that when the cytotoxicity results are conventionally presented as percentage cell viability, some data at the start point of the assay are lost.

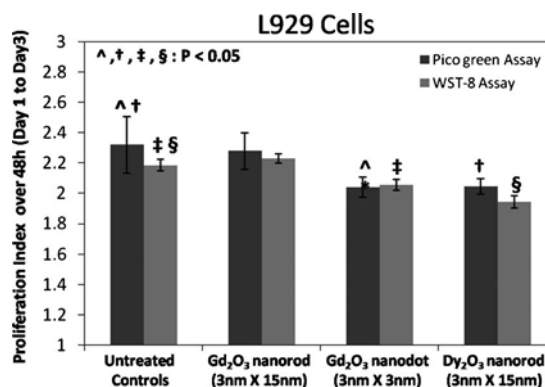


Fig. 9. Proliferation rates of L929 cells following trypsinization and reseeding on new culture plates after 48 h of pre-exposure to 2000 µg/ml of Gd<sub>2</sub>O<sub>3</sub> and Dy<sub>2</sub>O<sub>3</sub> nanoparticles.

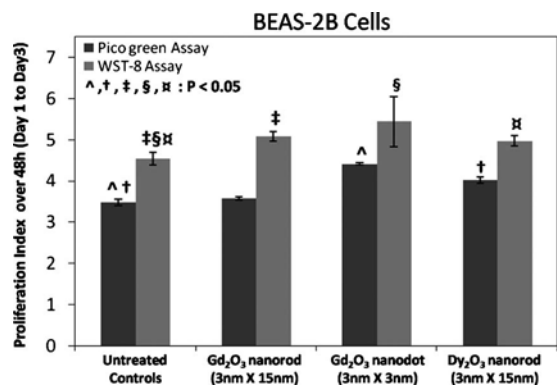


FIG. 10. Proliferation rates of BEAS-2B cells following trypsinization and reseeding on new culture plates after 48 h of pre-exposure to 2000  $\mu\text{g}/\text{ml}$  of  $\text{Gd}_2\text{O}_3$  and  $\text{Dy}_2\text{O}_3$  nanoparticles.

Both WST-8 and Pico-Green assays demonstrated that the  $\text{Dy}_2\text{O}_3$  nanorods were consistently less cytotoxic than either the  $\text{Gd}_2\text{O}_3$  nanorods or nanodots, for both L929 and BEAS-2B cells. To our knowledge, this study is the first-reported systematic comparison of the toxicity of  $\text{Gd}_2\text{O}_3$  and  $\text{Dy}_2\text{O}_3$  nanoparticles. Previously, in separate studies, it was reported that the  $\text{LD}_{50}$  of dysprosium chloride *in vivo* was 550 mg/kg of body mass,<sup>25</sup> which is marginally lower than the corresponding value of 585 mg/kg of body mass that was reported for gadolinium chloride.<sup>26</sup> Additionally, the cytotoxicity data with both assay methods also showed that  $\text{Gd}_2\text{O}_3$  nanodots were consistently more toxic than  $\text{Gd}_2\text{O}_3$  nanorods for L929 cells. For BEAS-2B cells, the results are less conclusive, with only the WST-8 assay demonstrating greater toxicity of  $\text{Gd}_2\text{O}_3$  nanodots versus nanorods, but with the Pico-Green assay showing no significant differences. The dimensions of nanorods are approximately  $3 \times 15 \text{ nm}^2$ , as compared to the nanodots that have an approximate dimension of  $3 \times 3 \text{ nm}^2$ . Thus, for any given mass or concentration, we would expect there to be 5 to 6 times more nanodots compared to nanorods that can potentially interact with the cell membrane and be internalized within the cell, hence the observed greater toxicity per unit mass of nanodots compared to nanorods.

A major deficiency of metabolism-based assays for cell viability determination is that the cytotoxicity data may be skewed by the differential effects of various nanomaterials on cellular metabolism. Hence, this study compared different methods of cytotoxicity assessment of the Tb-doped  $\text{Gd}_2\text{O}_3$  and  $\text{Dy}_2\text{O}_3$  nanoparticles, in particular, DNA quantification [Pico-Green versus metabolic (WST-8) assays]. Because the cytotoxic effects of these lanthanide nanomaterials were more pronounced at higher concentrations (Figs. 3 and 4), the comparison between Pico-Green and WST-8 assay was only done at the higher concentration points of 1000 and 2000  $\mu\text{g}/\text{ml}$ . Indeed, the results demonstrated much discrepancy in the cytotoxicity data obtained by the two different assay methods. This is consistent with the previous study of Shappell<sup>21</sup> that reported significant discrepancies in the cytotoxicity data obtained by DNA quantification versus metabolic assays, in the case of the soluble toxin ergovaline

on CACO-2 cells. Additionally, the study of Ng *et al.*,<sup>27</sup> which compared various DNA quantification and metabolic assays for measuring cell proliferation within two- and three-dimensional cultures, also showed much discrepancy in the data obtained by different assay methods.

Interestingly, it was observed for L929 cells that the values of proliferation index (48 h) obtained with the Pico-Green assay were consistently higher than the corresponding values of proliferation index obtained with the WST-8 assay (Fig. 5), whereas BEAS-2B cells displayed the opposite trend (Fig. 6). This would imply that for L929 cells, exposure to  $\text{Gd}_2\text{O}_3$  and  $\text{Dy}_2\text{O}_3$  nanoparticles decreased cellular metabolic activity, whereas for BEAS-2B cells, exposure to these nanoparticles led instead to an increase in metabolic activity. However, upon examining the untreated controls of both L929 and BEAS-2B cells (Figs. 5 and 6), the WST-8 assay consistently yielded significantly higher ( $P < 0.05$ ) values of proliferation index compared to the Pico-Green assay. It is hypothesized that there could be a lag-phase in cellular metabolic activity as the newly seeded trypsinized cells adhere to new culture plates on day 1, while on day 3, cellular metabolic activity gradually begins to pick up, in the absence of any toxic challenge for the untreated controls. Hence, it is apparent that  $\text{Gd}_2\text{O}_3$  and  $\text{Dy}_2\text{O}_3$  nanoparticles exert differential effects on the metabolic activity of BEAS-2B and L929 cells. The putative “proliferation index” calculated from absorbance readings of the WST-8 assay (as widely reported in most studies) should therefore be more appropriately labeled as “metabolism index.” Currently, metabolic assays such as WST-8, MTT, and MTS are still widely employed to quantify cell viability and proliferation rate under varying experimental conditions, with scant regard being given to differences in cellular metabolism between the experimental and control groups. It is often erroneously assumed that the cellular metabolic activity of the treatment and reference control groups are equivalent in the computation of cell viability and proliferation rates with WST-8, MTT, and MTS assays. Thus, these findings will cause a major rethinking of whether DNA-quantification assays have an advantage over metabolism-based assays in cytotoxicity assessment, simply because DNA quantification is not susceptible to being skewed by differential effects of nanomaterials on cellular metabolic activity.

Most of the previous studies on nanomaterial cytotoxicity did not further investigate cell biology and physiology after nanoparticle exposure. It must be noted that the confocal microscopy images (Figs. 7 and 8) confirmed that these lanthanide nanomaterials were still present within the cell cytoplasm 24 h after trypsinization and replating of the pre-exposed L929 and BEAS-2B cells. Given the utility of the  $\text{Gd}_2\text{O}_3$  and  $\text{Dy}_2\text{O}_3$  nanoparticles as bioimaging probes, it is therefore of clinical significance to evaluate whether these nanoparticles have any adverse postexposure effects. This study therefore evaluated the postexposure proliferation rates of both L929 and BEAS-2B cells. Interestingly, the results showed that prior exposure to  $\text{Gd}_2\text{O}_3$  and  $\text{Dy}_2\text{O}_3$  nanoparticles led to an increase in the proliferation rates of

BEAS-2B cells, whereas the opposite trend was observed with L929 cells (Figs. 9 and 10). These could arise from the differential effects of these lanthanides on the metabolic activity of L929 and BEAS-2B cells. Comparison between the Pico-Green and WST-8 assays (Figs. 5 and 6) had shown that for L929 cells, exposure to  $Gd_2O_3$  and  $Dy_2O_3$  nanoparticles decreased cellular metabolic activity; whereas BEAS-2B cells exhibited the opposite trend. Hence, after 48 h exposure, followed by subsequent trypsinization and reseeded onto new culture plates, the decreased metabolic activity of the pre-exposed L929 cells may be manifested by slower proliferation compared to the untreated control (Fig. 9), while the increased metabolic activity of the pre-exposed BEAS-2B cells may instead be manifested as faster proliferation (Fig. 10). The detailed mechanisms underlying these observations are currently uncharacterized and will be the subject of future investigations.

In conclusion,  $Gd_2O_3$  nanoparticles exhibit higher toxicity than  $Dy_2O_3$  nanoparticles, and  $Gd_2O_3$  nanodots are generally more toxic than  $Gd_2O_3$  nanorods, even though the Pico-Green assay result with BEAS-2B cells was inconclusive. The postexposure proliferation data did not provide any conclusive evidence of which nanomaterial was more toxic than the others, besides the observation that prior exposure to these lanthanide nanomaterials led to significant changes in the postexposure proliferation rates of both L929 and BEAS-2B cells. Additionally, the results of this study would suggest a timely rethinking and reexamination of the conventional data presentation format and commonly used laboratory protocols for cytotoxic assessment of nanomaterials. In particular, three pertinent issues have to be addressed. First, the conventional format of presenting cytotoxicity data in terms of loss of cell viability may be inappropriate if there is in fact no net decrease in the absolute number of viable cells, such as in the case of mildly toxic nanomaterials. Second, metabolic assays may not be the most appropriate means of assessing cytotoxicity, given the possibility of the data being skewed by differential effects of nanomaterials on cellular metabolism. Lastly, it may be of clinical significance to evaluate the postexposure effects of certain nanomaterials on cell biology and physiology.

- <sup>1</sup>G. K. Das *et al.*, *Langmuir* **26**, 8959 (2010).
- <sup>2</sup>G. K. Das and T. T. Tan, *J. Phys. Chem. C* **112**, 11211 (2008).
- <sup>3</sup>L. Q. Xiong, Z. G. Chen, M. X. Yu, F. Y. Li, C. Liu, and C. H. Huang, *Biomaterials* **30**, 5592 (2009).
- <sup>4</sup>H. G. Kang, F. Tokumasu, M. Clarke, Z. Zhou, J. Tang, T. Nguyen, and J. Hwang, *Wiley Interdiscip Rev Nanomed Nanobiotechnol.* **2**, 48 (2010).
- <sup>5</sup>C. Walkey, E. A. Sykes, and W. C. Chan, *Hematology Am Soc Hematol Educ Program* **2009**, 701 (2009).
- <sup>6</sup>R. J. Palmer, J. L. Butenhoff, and J. B. Stevens, *Environ. Res.* **43**, 142 (1987).
- <sup>7</sup>S. Heer, K. Kompe, H. U. Gudel, and M. Haase, *Adv. Mater.* **16**, 2102 (2004).
- <sup>8</sup>D. R. Larson, W. R. Zipfel, R. M. Williams, S. W. Clark, M. P. Bruchez, F. W. Wise, and W. W. Webb, *Science* **300**, 1434 (2003).
- <sup>9</sup>S. Aime, D. D. Castelli, S. G. Crich, E. Gianolio, and E. Terreno, *Acc. Chem. Res.* **42**, 822 (2009).
- <sup>10</sup>E. Pérez-Mayoral, V. Negri, J. Soler-Padrós, S. Cerdán, and P. Ballesteros, *Eur. J. Radiol.* **67**, 453 (2008).
- <sup>11</sup>C. M. Spangler, C. Spangler, and M. Schäerling, *Ann. N.Y. Acad. Sci.* **1130**, 138 (2008).
- <sup>12</sup>J. Cheon and J. H. Lee, *Acc. Chem. Res.* **41**, 1630 (2008).
- <sup>13</sup>M. Bottrill, L. Kwok, and N. J. Long, *Chem. Soc. Rev.* **35**, 557 (2006).
- <sup>14</sup>M. Norek, E. Kampert, U. Zeitler, and J. A. Peters, *J. Am. Chem. Soc.* **130**, 5335 (2008).
- <sup>15</sup>G. K. Das, P. P. Chan, A. Teo, J. S. Loo, J. M. Anderson, and T. T. Tan, *J. Biomed. Mater. Res. Part A* **93**, 337 (2010).
- <sup>16</sup>M. M. Nociari, A. Shalev, P. Benias, and C. Russo, *J. Immunol. Methods* **213**, 157 (1998).
- <sup>17</sup>S. Setua, D. Menon, A. Asok, S. Nair, and M. Koyakutty, *Biomaterials* **31**, 714 (2010).
- <sup>18</sup>T. Mosmann, *J. Immunol. Methods* **65**, 55 (1983).
- <sup>19</sup>G. Malich, B. Markovic, and C. Winder, *Toxicology* **124**, 179 (1997).
- <sup>20</sup>M. Ishiyama, Y. Miyazono, K. Sasamoto, Y. Ohkura, and K. Ueno, *Talanta* **44**, 1299 (1997).
- <sup>21</sup>N. W. Shappell, *In Vitro Cell. Dev. Biol.: Anim.* **39**, 329 (2003).
- <sup>22</sup>Y. Zhang, G. K. Das, R. Xu, and T. T. Tan, *J. Mater. Chem.* **19**, 3696 (2009).
- <sup>23</sup>J. K. Jaiswal, H. Mattoussi, J. M. Mauro, and S. M. Simon, *Nat. Biotechnol.* **21**, 47 (2003).
- <sup>24</sup>X. Wu, H. Liu, J. Liu, K. N. Haley, J. A. Treadway, J. P. Larson, N. Ge, F. Peale, and M. P. Bruchez, *Nat. Biotechnol.* **21**, 41 (2003).
- <sup>25</sup>T. J. Haley, K. Raymond, N. Komesu, and H. C. Upham, *Br J Pharmacol Chemother* **17**, 526 (1961).
- <sup>26</sup>T. J. Haley, L. Koste, N. Komesu, M. Efros, and H. C. Upham, *Toxicol. Appl. Pharmacol.* **8**, 37 (1966).
- <sup>27</sup>K. W. Ng, D. T. Leong, and D. W. Hutmacher, *Tissue Eng.* **11**, 182 (2005).